Ru valence in $RuSr_2Gd_{2-x}Ce_xCu_2O_{10+\delta}$ as measured by x-ray-absorption near-edge spectroscopy

G. V. M. Williams
2. Physikalisches Institut, Universität Stuttgart, D-70550 Stuttgart, Germany

L.-Y. Jang
Synchrotron Radiation Research Center (SRRC), Hsinchu, Taiwan, Republic of China

R. S. Liu
Department of Chemistry, National Taiwan University, Taipei, Taiwan, Republic of China
(Received 15 June 2001; published 16 January 2002)

We report the results from x-ray-absorption near-edge spectroscopy, electrical resistance, and thermopower measurements on $RuSr_2Gd_{2-x}Ce_xCu_2O_{10+\delta}$. This compound displays the coexistence of superconductivity and ferromagnetic order. Furthermore, there are systematic changes in the temperature dependence of the magnetization with increasing Ce concentration. However, we find from our study that the average Ru valence is 4.95 ± 0.05 irrespective of the Ce concentration. This implies that there is no charge transfer to the RuO_2 layer with increasing Ce concentration. The nearly constant superconducting transition temperature for $0.6 \leqslant x \leqslant 0.8$ indicates that there is also no significant charge transfer to the CuO_2 planes even though Ce^{4+} is expected to decrease the hole concentration by 0.1. It is possible that the decrease in the hole concentration is compensated for by an increase in the oxygen content δ.

DOI: 10.1103/PhysRevB.65.064508 PACS number(s): 74.72.−h, 74.25.Jb, 74.25.Fy

INTRODUCTION

It has recently been shown that superconductivity and ferromagnetic order coexist in $RuSr_2R_{2-x}Ce_xCu_2O_{10+\delta}$ (R = Gd, Eu),[1] where the magnetic ordering temperature is significantly greater than the superconducting transition temperature. This is particularly interesting because ferromagnetic order and superconductivity cannot coexist without some form of accommodation, for example, via a spatial modulation of the respective order parameters or via a spontaneous vortex phase.[2–4] It is believed that in the case of $RuSr_2R_{2-x}Ce_xCu_2O_{10+\delta}$ there exits a spontaneous vortex phase where the spontaneous magnetization gives rise to a local magnetic field, which is greater than B_{c1} for temperatures between T_{SVP} and T_c. For temperatures less than T_{SVP}, the spontaneous internal field is greater than B_{c1} and hence the Meissner phase develops.[2]

The hybrid ruthenate cuprates ($RuSr_2RCu_2O_8$ and $RuSr_2R_{2-x}Ce_xCu_2O_{10+\delta}$) are also interesting because they produce magnetic behavior not observed in other ruthenate compounds containing RuO_2 layers (e.g., $SrRuO_3$, Sr_2RRuO_6). For example, $RuSr_2GdCu_2O_8$ and $RuSr_2EuCu_2O_8$ are predominately antiferromagnetic in the low-field region and there is evidence of a spin-flop transition as the magnetic field is increased.[5–7] Interestingly, a recent powder neutron-diffraction study on $RuSr_2YCu_2O_8$ revealed low-field antiferromagnetic order with a significant ferromagnetic component.[8] However, as has been found in $RuSr_2GdCu_2O_8$ and $RuSr_2EuCu_2O_8$, the high-field magnetic order in $RuSr_2YCu_2O_8$ is ferromagnetic. It has recently been shown from an x-ray-absorption near-edge spectroscopy (XANES) study that, unlike other ruthenate compounds, $RuSr_2RCu_2O_8$ has a mixed Ru valence in the RuO_2 layers consisting of 38% (Ru^{4+}) and 62% (Ru^{5+}).[9] A similar conclusion was reached from a high-temperature susceptibility study of $RuSr_2RCu_2O_8$.[10] This can be contrasted with the ferromagnetic superconductor $RuSr_2Eu_{1.5}Ce_{0.5}Cu_2O_{10+\delta}$, where an x-ray-absorption (XAS) study indicated that the Ru valence is 5.0+.[11] Sr_2RRuO_6 also has a Ru valence of 5.0+ but it is antiferromagnetic.[12]

It is apparent in Fig. 1 that the unit cell of $RuSr_2Gd_{2-x}Ce_xCu_2O_{10+\delta}$ [based on that of $NbSr_2R_{2-x}Ce_xCu_2O_{10+\delta}$ (Ref. 13) and

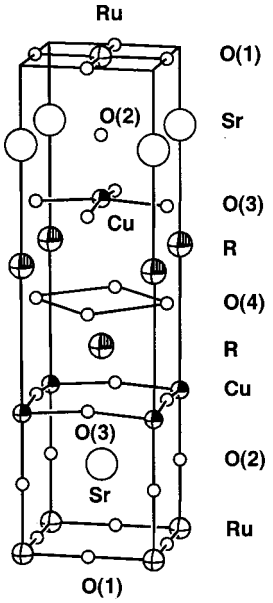

FIG. 1. Plot of one half of the $RuSr_2R_{2-x}Ce_xCu_2O_{10+\delta}$ unit cell based on the $NbSr_2R_{2-x}Ce_xCu_2O_{10+\delta}$ (Ref. 13) and $TaSr_2Nb_{2-x}Ce_xCu_2O_{10+\delta}$ (Ref. 14) analog.

$TaSr_2Nd_{2-x}Ce_xCu_2O_{10+\delta}$ (Ref. 14)] is different from $RuSr_2RCu_2O_8$. In particular, it contains the electron doped T' structure ($R_{2-x}Ce_xCuO_4$), separated by strontium oxide and ruthenium oxide layers. Furthermore, unlike $RuSr_2RCu_2O_8$, the adjacent RuO_2 layers in $RuSr_2Gd_{2-x}Ce_xCu_2O_{10+\delta}$ are shifted by ($a/2$,$a/2$) where a is the a,b lattice parameter. It should be noted that the RuO_6 octahedra in $RuSr_2GdCu_2O_8$ is known to be rotated by $\sim 14°$ about the c axis[15,16] and possibly tilted by $\sim 10°$.[15] Unfortunately, it is not known if a similar rotation and tilt of the RuO_6 octahedra occurs in $RuSr_2Gd_{2-x}Ce_xCu_2O_{10+\delta}$.

The understanding of $RuSr_2R_{2-x}Ce_xCu_2O_{10+\delta}$ is complicated by a recent study which has shown that the temperature where the peak in the zero-field-cooled magnetization data occurs, T_p, and the magnetization at 10 kG increase with increasing Ce concentration.[17] However, the superconducting transition temperature does not significantly change for $0.4 \leqslant x \leqslant 0.8$ and hence it is not clear what is happening to the additional carriers introduced by Ce substitution. It is not known if the systematic changes in T_p or the magnetization at 10 kG are correlated with a reduction in the Ru valence. In the case of $RuSr_2GdCu_2O_8$, it has been found that the substitution of Dy for Gd or Ba for Sr results in significant changes in the average Ru valence, the superconducting transition temperature and the magnetic order.[9] It is therefore important to perform a study on $RuSr_2Gd_{2-x}Ce_xCu_2O_{10+\delta}$ with different Ce concentrations to see if the changes in the magnetic and superconducting order are also correlated with changes in the Ru valence.

In this paper, we report a systematic XANES study on $RuSr_2Gd_{1-x}Ce_xCu_2O_{10+\delta}$ with $0.6 \leqslant x \leqslant 1.0$. We show below that the average Ru valence is near 5.0, indicating that there is no charge transfer to the RuO_2 layers with increasing Ce concentration.

EXPERIMENTAL DETAILS

The $RuSr_2Gd_{2-x}Ce_xCu_2O_{10+\delta}$ ceramic samples were made by first decomposing a stoichiometric mix of RuO_2, $Sr(CO_3)_2$, Gd_2O_3, CeO_2, and CuO in air at 960 °C. The powder was pressed into pellets an then sintered at 1010 °C in flowing N_2 for 10 h to suppress the growth of $SrRuO_3$. This process results in Sr_2GdRuO_6, CeO_2, and CuO. The pellets were ground, pressed and sintered at 1065 °C for 10 h in flowing O_2. This was followed by additional grinding and sintering at 1070 °C for 10 h and 1070 °C for five days. The samples were air quenched after each sintering step. The samples were then oxygen loaded at 100 bars at 600 °C for 12 h, ramped to 350 °C over 24 h and then held at 350 °C for 72 h. There was no evidence of the main impurity phases in the x-ray-diffraction spectra.

The ac susceptibility measurements were made using a superconducting quantum interference device magnetometer and a frequency of 1 kHz with an ac magnetic field of 0.05 G. Variable temperature four terminal resistance measurements were made in the temperature range of 5–280 K and room-temperature thermopower measurements were made using the standard differential temperature technique.

The XANES experiments were performed on beamline BL15B at SRRC in Hsinchu, Taiwan by using a double crystal Si(111) monochromator. The Ru L_{III}-edge measurements were carried out in fluorescence mode at room temperature using a modified Lytle detector. The energy calibration was performed by using the L_{II}- and L_{III}-edge features of Mo and Pd metallic foils. The estimated energy resolution was 0.47 eV at the Ru L_{III} edge. The background was subtracted using the program AUTOBK.[18]

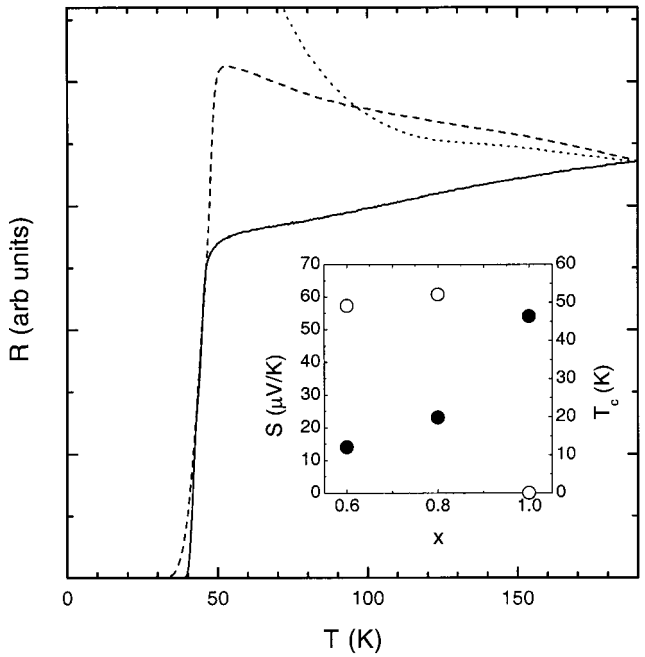

FIG. 2. Plot of the resistance against temperature from $RuSr_2Gd_{2-x}Ce_xCu_2O_{10+\delta}$ with $x=0.6$ (solid curve), $x=0.8$ (dashed curve), and $x=1.0$ (dotted curve) normalized to the same resistance at 180 K. Inset: Plot of the room-temperature thermopower against Ce concentration (solid circles and left axis) and the superconducting transition temperature against Ce concentration (open symbols and right axis).

RESULTS AND ANALYSES

We present in Fig. 2 the normalized resistance curves for our $RuSr_2Gd_{2-x}Ce_xCu_2O_{10+\delta}$ samples. It is apparent that only the $x=0.6$ and $x=0.8$ samples are superconducting. This is consistent with previous studies, which found superconductivity for x in the range $0.4 \leqslant x \leqslant 0.8$,[1,17,19] and that there is no significant change in T_c for Ce concentrations within this range.[17] The superconducting transition temperatures are plotted in the inset to Fig. 2 (open circles and right axis). We define the superconducting transition temperature using the same criteria used in previous studies on $RuSr_2RCu_2O_8$ and $RuSr_2R_{2-x}Ce_xCu_2O_{10+\delta}$ where the superconducting transition temperature is the temperature where the resistance begins to decrease.[17,20–22] The maximum superconducting transition temperatures are comparable to those found in previous studies.[1,17,19]

The room-temperature thermopower S (293 K) increases with increasing Ce concentration as can be seen in the inset to Fig. 2 (filled circles and left axis). These values can be

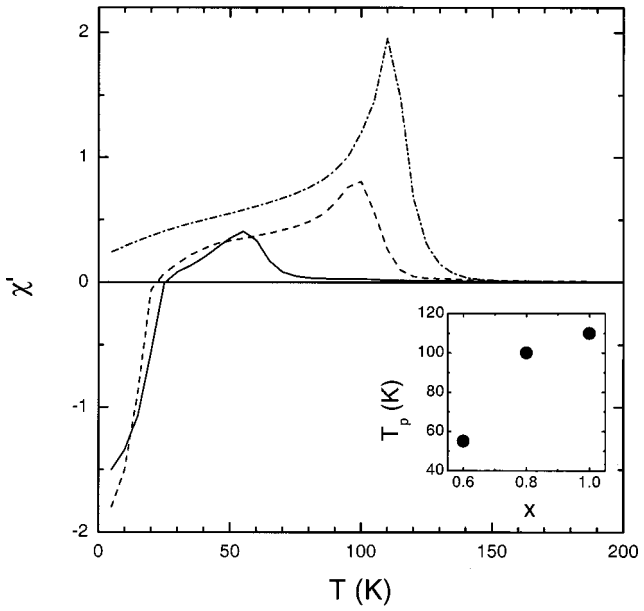

FIG. 3. Plot of the zero-field ac susceptibility against temperature for $RuSr_2Gd_{2-x}Ce_xCu_2O_{10+\delta}$ with $x=0.6$ (solid curve), $x=0.8$ (dashed curve), and $x=1.0$ (dot-dashed curve). Note that data have not been corrected for demagnetizing effects. Inset: Plot of the peak in the zero-field ac susceptibility T_p against Ce concentration.

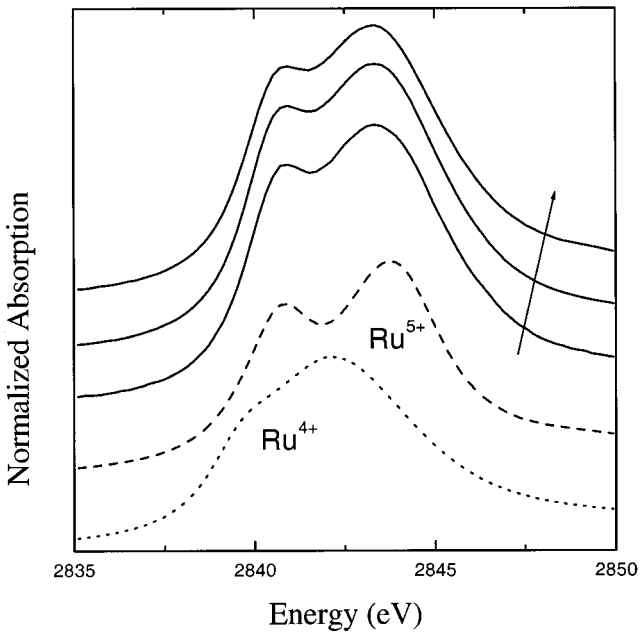

FIG. 4. Plot of the XANES spectra for $RuSr_2Gd_{2-x}Ce_xCu_2O_{10+\delta}$ with $x=0.6$, 0.8, and 1.0 (solid curves), $SrRuO_3$ [dotted curve (Ref. 9)], and Sr_2GdRuO_6 [dashed curve (Ref. 9)]. The arrow indicates increasing Ce concentration.

compared with those measured in the high-temperature superconducting cuprates (HTSC's) where it has been found that there is a good correlation between S (293 K) and hole concentration on the CuO_2 planes for most of the HTSC's.[23] In particular, S (293 K) is greater than ~ 1 μV/K for underdoped HTSC's and S (293 K) is less than ~ 1 μV/K for overdoped HTSC's. Thus S (293 K) measured in $RuSr_2R_{2-x}Ce_xCu_2O_{10+\delta}$ indicates that these compounds are underdoped. Based on the correlation between S (293 K) and hole concentration found in the HTSC's, we might expect that the $x=0.8$ sample should have a lower hole concentration and hence a T_c value less than that found in the $x=0.6$ sample. However, it is apparent in the inset to Fig. 2 that this is not the case. It may be that there is an additional contribution from the RuO_2 layers or, like $La_{2-x}Sr_xCuO_4$, $RuSr_2R_{2-x}Ce_xCu_2O_{10+\delta}$ does not exactly follow the correlation between S (293 K) and hole concentration found in the HTSC's.

It can be seen in Fig. 2 that the zero resistance temperature $T_c(0)$ is significantly less than T_c. This is also observed in $RuSr_2RCu_2O_8$ and it is a consequence of the spontaneous vortex phase.[2,4,20–22] The onset of the diamagnetic transition near $T_{SVP}=24$ K for $0.6\leqslant x\leqslant 0.8$ can be seen in the zero-field ac susceptibility data plotted in Fig. 3. We note that, unlike similar measurements on $RuSr_2EuCu_2O_8$, T_{SVP} is consistently lower than the zero resistance temperature $T_c(0)$. This could be due to freezing of the flux lattice occurring at a temperature greater than T_{SVP} in $RuSr_2Gd_{2-x}Ce_xCu_2O_{10+\delta}$.

The ac susceptibility data also display a peak at T_p for temperatures greater than T_{SVP}. This peak corresponds to the temperature where the maximum negative derivative of the dc magnetization in an applied field of 50 G is observed. Therefore we associate it with magnetic ordering in the RuO_2 layers. We have previously shown that T_p decreases with increasing oxygen content and hence T_p observed in the current samples is lower than in the previous samples.[17] It can be seen in the inset to Fig. 3 that there is an increase in T_p with increasing Ce concentration, which will be discussed later.

The invariance of T_c and T_{SVP} to x for x in the range $0.6\leqslant x\leqslant 0.8$ is surprising and indicates that there is no significant change in the hole concentration on the CuO_2 planes. However, the increase in x from 0.6 to 0.8 should result in a decrease in the hole concentration of 0.10 per CuO_2 plane and, by comparison with other HTSC's,[24] should lead to a rapid decrease in T_c. It is possible that the decreasing hole concentration is being offset by an increase in δ. We note that a similar effect is observed in $Bi_2Sr_2Ca_{1-x}Y_xCu_2O_{8+\delta}$ where T_c is nearly independent of hole concentration for $0\leqslant x\leqslant 0.5$ and δ increases by ~ 0.38 when y is increased from 0 to 1.[25] Unfortunately, there are no reports of the oxygen content in $RuSr_2Gd_{2-x}Ce_xCu_2O_{10+\delta}$. We note that an increase in the oxygen content in $RuSr_2Gd_{2-x}Ce_xCu_2O_{10+\delta}$ of only 0.10 as x is increased from 0.6 to 0.8 would be sufficient to compensate for the additional carriers introduced by Ce.

The assumption that an increasing Ce concentration is compensated for by a corresponding increase in δ depends on there being no charge transfer to the RuO_2 layers. However, it is apparent in Fig. 4 that the Ru valence does not change with increasing Ce concentration. Here we plot the L_{III}-edge XANES spectra from $RuSr_2Gd_{2-x}Ce_xCu_2O_{10+\delta}$ for different Ce concentrations. The XANES spectra can be understood by noting that the octahedral crystal field splits

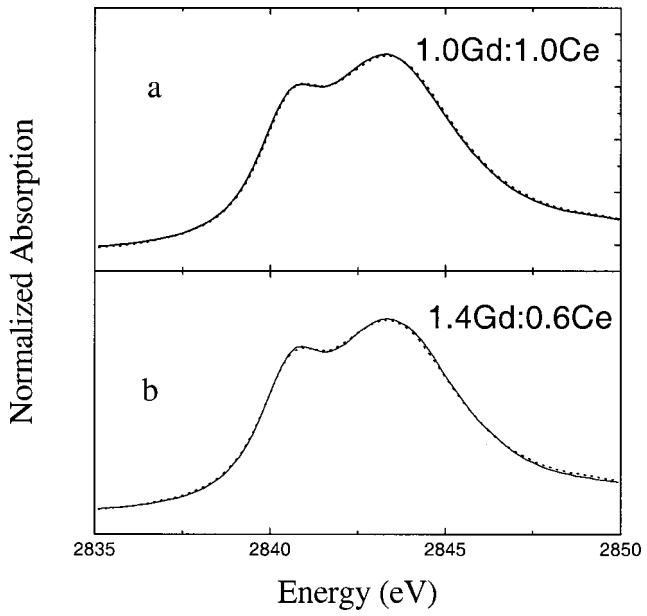

FIG. 5. Plot of the XANES spectra for $RuSr_2R_{2-x}Ce_xCu_2O_{10+\delta}$ (solid curves) with $x=1.0$ (a) and $x=0.6$ (b). Also plotted is a fit to the data using the $SrRuO_3$ and Sr_2GdRuO_6 XANES spectra (dotted curves) as described in the text.

the Ru $4d$ states into t_{2g} and e_g levels. The inclusion of additional spin-orbit splitting and a weak tetragonal distortion results in the splitting of the t_{2g} level into three levels and the e_g level into two levels.[26] Thus the lower energy peak corresponds to a $2p \rightarrow t_{2g}$ transition and the higher energy peak corresponds to a $2p \rightarrow e_g$ transition.[26]

The average Ru valence can be obtained by comparing the $RuSr_2Gd_{2-x}Ce_xCu_2O_{10+\delta}$ XANES spectra with that from $SrRuO_3$ (Ru^{4+}) (Ref. 9) and Sr_2GdRuO_6 (Ru^{5+}) (Ref. 9) which are also plotted in Fig. 4. A previous XANES study of $RuSr_2GdCuO_8$ found that the XANES spectra could be fitted to a linear combination of the $SrRuO_3$ (Ru^{4+}) and Sr_2GdRuO_6 (Ru^{6+}) XANES spectra.[9] As mentioned above, in the case of $RuSr_2GdCuO_8$ it was found that XANES spectra could be fitted to 38% Ru^{4+} and 62% Ru^{5+} and that the average Ru valence changed with the substitution of Dy on the Gd site or Ba on the Sr site.[9] However, it is apparent in Fig. 4 that the XANES spectra from $RuSr_2Gd_{2-x}Ce_xCu_2O_{10+\delta}$ is independent of the Ce concentration for $0.6 \leqslant x \leqslant 1.0$ and the Ru valence is close to 5. This is clearer in Fig. 5 where we plot the XANES spectra from $RuSr_2Gd_{2-x}Ce_xCu_2O_{10+\delta}$ with $x=1.0$ [Fig. 5(a)] and $x=0.6$ [Fig. 5(b)]. Also plotted is a linear combination of 5% of the $SrRuO_3$ (Ru^{4+}) and 95% of the Sr_2GdRuO_6 (Ru^{5+}) XANES spectra (dotted curves). We find that the average Ru valence is 0.95 ± 0.05 and independent of the Ce concentration.

A previous study found that the Ru valence is near 5 for $x=0.5$.[11] Thus it is apparent that there is no change in the Ru valence over a large Ce concentration range, spanning $x=0.5-1$, even though the superconducting transition temperature is essentially constant for x in the range $0.5 \leqslant x \leqslant 0.8$.[17] This indicates that the substitution of the smaller Ce^{4+} ion [ionic radii $=0.97$ Å (Ref. 27)] for the larger Gd^{3+} ion [ionic radii $=1.053$ Å (Ref. 27)] is not resulting in a significant charge transfer to the CuO_2 planes or the RuO_2 planes. However, a similar study of $RuSr_2Gd_{0.6}Dy_{0.4}Cu_2O_8$ found that the isoelectronic substitution of the smaller Dy^{3+} ion [ionic radii $=1.027$ Å (Ref. 27)] for the larger Gd^{3+} ion resulted in an increase in the hole concentration on the CuO_2 planes and a decrease in the average Ru valence.[9] Therefore as mentioned above, it is possible that electron doping by Ce^{4+} in $RuSr_2Gd_{2-x}Ce_xCu_2O_{10+\delta}$ is being partially compensated for by a corresponding increase in δ. The location of the additional oxygen sites is not clear. However, $RuSr_2Gd_{2-x}Ce_xCu_2O_{10+\delta}$ contains the $RuSr_2GdCu_2O_8$ substructure which is known to be stoichiometric[20] and hence it may be that the additional oxygen is located in the GdO layers.

As mentioned earlier, it is apparent in Fig. 3 that T_p increases with increasing Ce concentration while, as we have shown above, there is no corresponding change in the Ru valence. This is interesting because the isoelectronic substitution of Ba^{2+} for Sr^{2+} or Dy^{3+} for Gd^{3+} in $RuSr_2GdCu_2O_8$ results in a change in the magnetic order and the Ru valence.[9] In the absence of systematic structural data, we suggest that the increasing T_p is due to structural changes as well as a change in the c-axis exchange energy. We note that systematic changes in the magnetic ordering temperature are also observed in $Sr_{1-x}Ca_xRuO_3$ which has been classified as a bandwidth-controlled Mott-Hubbard system[28] where the ferromagnetic ordering temperature systematically decreases with increasing Ca concentration.[29,30] A computational study has shown that the situation is more complicated because the increasing RuO_6 octahedral distortions with increasing Ca concentration lead to a narrowing of the t_{2g} band but the appearance of pseudogaps for high Ca concentrations leads to broadening of the t_{2g} band.[31] These competing effects eventually lead to a ferromagnetically correlated metal for high Ca concentrations where the increasing RuO_6 octahedral distortions are driven by the decrease in the ionic radii of Ca^{2+} when compared with Sr^{2+}.[30] It is therefore possible that the changes in T_p observed in $RuSr_2Gd_{2-x}Ce_xCu_2O_{10+\delta}$ are due to similar competing effects as well as possible changes in the c-axis coupling energy between the RuO_2 layers.

CONCLUSION

In conclusion, we find that the XANES spectra from $RuSr_2Gd_{2-x}Ce_xCu_2O_{10+\delta}$ can be decomposed into $95 \pm 5\%$ Ru^{5+} and $5 \pm 5\%$ Ru^{4+} irrespective of the Ce concentration. This is consistent with there being no charge transfer to the RuO_2 layers. Furthermore, there is no significant charge transfer to the CuO_2 planes for $0.6 \leqslant x \leqslant 0.8$. This can be contrasted with the isoelectronic substitution of Ba for Sr or Dy for Gd in $RuSr_2GdCu_2O_8$ where there is charge transfer to the CuO_2 planes and significant changes in the average Ru valence. We speculate that the electrons introduced by Ce in $RuSr_2Gd_{2-x}Ce_xCu_2O_{10+\delta}$ are compensated for by an increase in the oxygen content.

ACKNOWLEDGMENTS

We acknowledge funding support from the National Science Council of the Republic of China NSC under Grant No. 89-2113-M-002-059 (R.S.I.), the New Zealand Marsden Fund (G.V.M.W.), and the Alexander von Humboldt Foundation (G.V.M.W.). We acknowledge helpful discussions with S. Krämer.

[1] A. Felner, U. Asaf, Y. Lavi, and O. Milio, Phys. Rev. B **55**, 3374 (1997).
[2] E. B. Sonin and I. Felner, Phys. Rev. B **57**, 14 000 (1998).
[3] W. E. Picket, R. Weht, and A. B. Shick, Phys. Rev. Lett. **83**, 3713 (1999).
[4] C. Bernhard, J. L. Tallon, E. Bruecher, and K. K. Kremer, Phys. Rev. B **61**, 14 960 (2000).
[5] J. W. Lynn, B. Keimer, C. Ulrich, C. Bernhard, and J. L. Tallon, Phys. Rev. B **61**, 14 964 (2000).
[6] J. D. Jorgensen, O. Chmaissem, H. Shaked, S. Short, P. W. Klamut, B. Dabrowski, and J. L. Tallon, Phys. Rev. B **63**, 054440 (2001).
[7] G. V. M. Williams and S. Krämer, Phys. Rev. B **62**, 4132 (2000).
[8] H. Takagawi, J. Akimitsu, H. Kawano-Furukawa, and H. Yoshizawa, J. Phys. Soc. Jpn. **70**, 333 (2001).
[9] R. S. Liu, L.-Y. Jang, H.-H. Hung, and J. L. Tallon, Phys. Rev. B **63**, 212507 (2001).
[10] A. Butera, A. Fainstein, E. Winkler, and J. L. Tallon, Phys. Rev. B **63**, 054442 (2001).
[11] I. Felner, U. Asaf, C. Godart, and E. Alleno, Physica B **259–261**, 703 (1999).
[12] P. D. Battle and C. W. Jones, J. Solid State Chem. **78**, 108 (1989); Y. Doi and Y. Hinatsu, J. Phys.: Condens. Matter **11**, 4813 (1999).
[13] L. Rukang, Z. Yingjie, Q. Yitai, and L. Zuyao, Physica C **176**, 19 (1991).
[14] T. J. Goodwin, H. B. Radousky, and R. N. Shelton, Physica C **204**, 212 (1992).
[15] A. C. McLaughlin, W. Zhou, J. P. Attfield, A. N. Fitch, and J. L. Tallon, Phys. Rev. B **60**, 7512 (1999).
[16] O. Chmaissem, J. D. Jorgensen, H. Shaked, P. Dollar, and J. L. Tallon, Phys. Rev. B **61**, 6401 (2000).
[17] G. V. M. Williams and M. Ryan, Phys. Rev. B **64**, 094515 (2001).
[18] N. Newville, P. Livins, Y. Yacoby, J. J. Rehr, and E. A. Stern, Phys. Rev. B **47**, 14 126 (1993).
[19] L. Bauernfeind, W. Widder, and H. F. Braun, Physica C **254**, 151 (1995).
[20] J. Tallon, C. Bernhard, M. Bowden, P. Gilberd, T. Stoto, and D. Pringle, IEEE Trans. Appl. Supercond. **9**, 1051 (1999).
[21] C. Bernhard, J. L. Tallon, Ch. Neidermayer, Th. Blasius, A. Golnik, E. Brücher, R. K. Kremer, D. R. Noakes, C. E. Stronach, and E. J. Ansaldo, Phys. Rev. B **59**, 14 099 (1999).
[22] J. L. Tallon, J. W. Loram, G. W. M. Williams, and C. Bernhard, Phys. Rev. B **61**, 6471 (2000).
[23] S. D. Obertelli, J. R. Cooper, and J. L. Tallon, Phys. Rev. B **46**, 14 928 (1992).
[24] M. R. Presland, J. L. Tallon, R. G. Buckley, R. S. Liu, and N. E. Flower, Physica C **176**, 95 (1991).
[25] W. A. Groen, D. M. de Leeuw, and L. F. Feiner, Physica C **165**, 55 (1990).
[26] Z. Hu, H. von Lips, M. S. Golden, J. Fink, G. Kaindl, F. M. F. de Groot, S. Ebbinghaus, and A. Reller, Phys. Rev. B **61**, 5262 (2000).
[27] R. D. Shannon, Acta Crystallogr., Sect. A: Cryst. Phys., Diffr., Theor. Gen. Crystallogr. **32**, 751 (1976).
[28] J. S. Ahn, J. Bak, H. S. Choi, T. W. Noh, Y. Bang, J. H. Cho, and Q. X. Jia, Phys. Rev. Lett. **82**, 5321 (1999).
[29] G. Cao, S. McCall, M. Shepard, J. E. Crow, and R. P. Guertin, Phys. Rev. B **56**, 312 (1997).
[30] K. Yoshimura, T. Imai, T. Kiyama, K. R. Thurber, A. W. Hunt, and K. Kosuge, Phys. Rev. Lett. **83**, 4397 (1999).
[31] I. I. Mazin and D. J. Singh, Phys. Rev. B **56**, 2556 (1997).